Magnetostatic-Wave Envelope Soliton in Microstrip Line Using YIG-Film Substrate

Makoto Tsutsumi, *Senior Member, IEEE,* Tetsuya Ueda, *Member, IEEE,* and Kensuke Okubo, *Member, IEEE*

***Abstract*—In this paper, a dispersion relation of the microstrip line on a yttrium–iron–garnet (YIG)-film substrate has been derived under the approximation of a two-dimensional analysis. The dispersion curve shows the mixed state of quasi-TEM mode and magnetostatic forward volume wave (MSFVW) mode, and these two modes are coupled with each other at gyromagnetic frequency where MSFVW solitons are excited efficiently. Based on the numerical parameters of the calculated dispersion curve, simulation of the soliton form has been carried out by numerically solving the nonlinear Schrödinger equation. The results are compared with the experimental results of MSFVW envelope bright soliton in a microstrip line on YIG-film–gadolinium–gallium–garnet substrate.**

***Index Terms*—Magnetostatic waves, microstrip line, microwave soliton, nonlinear phenomenon, YIG film.**

I. Introduction

MAGNETOSTATIC wave (MSW) devices such as delay lines, filters, and resonators have been studied by many workers [1].

Recent interest of MSW devices is in nonlinear phenomena in a yttrium–iron–garnet (YIG)-film delay line at microwave frequency. Among them, MSW envelope soliton devices have been focused and actively studied by Russian scientists [2]–[4]. The potential applications of MSW envelope soliton such as pulse compression devices and soliton train generator are anticipated [5], [6]. The YIG-film delay line used for the envelope MSW soliton devices consists of a pair of transducers with input and output ports, as shown in Fig. 1(a), and these transducers are typically fabricated as a narrow microstrip line on a YIG film epitaxially grown on gadolinium–gallium–garnet (GGG) substrate, in which radiation of the MSW at the right angle to the strip line is emphasized in the analysis [7], [8].[1]

Recently, one of authors has experimentally demonstrated the MSW delay line using a microstrip line with a YIG-film–GGG substrate, as shown in Fig. 1(b), in which the MSW propagates along the microstrip line and the radiation effect at the right angle to the strip line is negligibly small for the wide strip width over 100 μm [9], [10]. Thus, it is noted that the microstrip-line-type delay line proposed here involves quite different mechanism (propagation problem) from the microstrip-type MSW transducer (excitation problem).

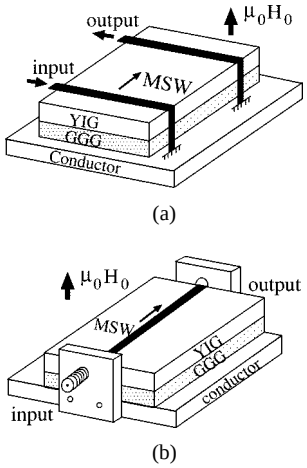

Fig. 1. Two types of MSW delay lines. (a) MSW waveguide with microstrip line type transducer. (b) Microstrip-type MSW waveguide.

This paper first investigates the dispersion relation of the microstrip line on a YIG-film–GGG substrate under the two-dimensional approximation analysis. Coupling between quasi-TEM and MSW modes is discussed in the dispersion curve, which characterizes the MSW delay lines in the linear state. The simulation of the MSW envelope soliton form is then provided based on the dispersion curve and compared with experimental results for a 20-μm-thick YIG-film substrate.

II. Theory on Dispersion Relation

The dispersion relation of the microstrip line on the YIG film and GGG layered substrate is derived in the linear state. To simplify the analyses and elucidate the fundamental aspect of the dispersion relation of the line, a two-dimensional theoretical model of the line is assumed in an infinite extent along the x- and y-directions, i.e., a parallel-plate model of the YIG-film waveguide, magnetized perpendicularly to the surface, as shown in Fig. 2.

Maxwell's equations in the ferrite medium are given by

$$\begin{aligned} \nabla \times \boldsymbol{H} &= j\omega\varepsilon_0\varepsilon_r \boldsymbol{E} \\ \nabla \times \boldsymbol{E} &= -j\omega\mu_0\hat{\mu}\boldsymbol{H}. \end{aligned} \tag{1}$$

The permeability tensor of YIG $\hat{\mu}$ in (1) is given by

$$\hat{\mu} = \begin{bmatrix} \mu & j\kappa & 0 \\ -j\kappa & \mu & 0 \\ 0 & 0 & 1 \end{bmatrix} \tag{2}$$

Manuscript received July 30, 1999.

M. Tsutsumi and T. Ueda are with the Faculty of Engineering and Design, Kyoto Institute of Technology, Matsugasaki, Kyoto 606-8585, Japan (e-mail: tutumi@dj.kit.ac.jp; ueda@dj.kit.ac.jp).

K. Okubo is with the Faculty of Computer Science and System Engineering, Okayama Prefectural University, Kuboki, Okayama 719-1197, Japan (e-mail: okubo@c.oka-pu.ac.jp).

Publisher Item Identifier S 0018-9480(00)00849-8.

[1]To estimate insertion loss of MSW transducer, a microstrip line with dielectric substrate has been assumed [7], [8].

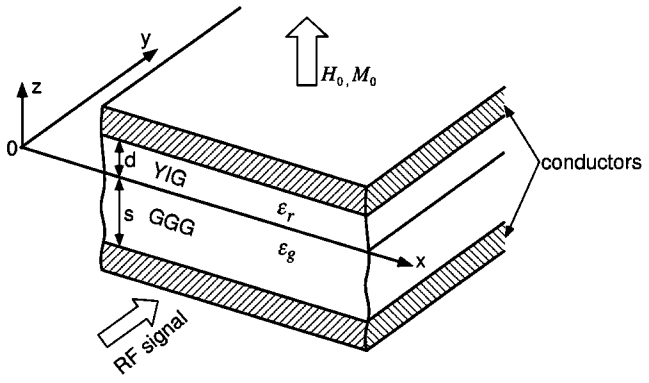

Fig. 2. Parallel-plate model of the microstrip line.

where $\mu = 1 + \omega_h\omega_m/(\omega_h^2 - \omega^2)$, $\kappa = \omega\omega_m/(\omega_h^2 - \omega^2)$, $\omega_h = \gamma\mu_0 H_0$, $\omega_m = \gamma\mu_0 M_0$, H_0 is the internal dc magnetic field, $\mu_0 M_0$ is the saturation magnetization, γ is the gyromagnetic ratio, and $\varepsilon_0\varepsilon_r$ is the dielectric constant of YIG [1].

The electromagnetic field in (1) is assumed to be independent of the x-direction. Even for the two-dimensional assumption, the electromagnetic field in (1) shows hybrid behavior with the differential equation in quadratic form as

$$\begin{aligned}
&\frac{\partial^2 E_y}{\partial z^2} - \left[\beta^2 - \varepsilon_r\mu\left(\frac{\omega}{c}\right)^2\right] E_y \\
&\quad = -\omega\mu_0\kappa\frac{\partial H_y}{\partial z} \\
&\frac{\partial^2 H_y}{\partial z^2} - \left[\beta^2 - \varepsilon_r\left(\frac{\omega}{c}\right)^2\right]\mu H_y \\
&\quad = \omega\varepsilon_0\varepsilon_r\kappa\frac{\beta^2 - \varepsilon_r\left(\frac{\omega}{c}\right)^2}{\beta^2 - \varepsilon_r\mu\left(\frac{\omega}{c}\right)^2}\left(\frac{\partial E_y}{\partial z} + \omega\mu_0\kappa H_y\right) \qquad (3)
\end{aligned}$$

where E_y and H_y vary with $e^{-j\beta y}$, and c is the speed of light in vacuum. Combining these two equations, we get

$$\begin{aligned}
&\frac{\partial^4 E_y}{\partial z^4} - \left\{(1+\mu)\beta^2 - 2\mu\varepsilon_r\left(\frac{\omega}{c}\right)^2\right\}\frac{\partial^2 E_y}{\partial z^2} \\
&\quad + \mu\left[\beta^2 - \varepsilon_r\left(\frac{\omega}{c}\right)^2\right]\left[\beta^2 - \varepsilon_r\mu_{ef}\left(\frac{\omega}{c}\right)^2\right] E_y \\
&\quad = 0, \\
&\mu_{ef} = \frac{\mu^2 - \kappa^2}{\mu}. \qquad (4)
\end{aligned}$$

The solution to (4) is given under the boundary condition at conductor $z = d$ in a simple form as

$$E_y = A_1\sinh\left[\lambda_p(z-d)\right] + A_2\sinh[\lambda_m(z-d)] \qquad (5)$$

$$\begin{aligned}
\lambda_p^2, \lambda_m^2 &= \frac{(1+\mu)\beta^2 - 2\mu\varepsilon_r\left(\frac{\omega}{c}\right)^2 \pm \sqrt{D}}{2} \\
D &= (1-\mu)^2\beta^4 - 4\varepsilon_r\left(\frac{\omega\kappa}{c}\right)^2\left[\beta^2 - \varepsilon_r\left(\frac{\omega}{c}\right)^2\right]
\end{aligned}$$

where A_1 and A_2 are arbitrary constants. Here, λ_p and λ_m may be complex. The RF magnetic field H_y in the ferrite can also be derived by combining (3) with (5).

The electromagnetic field in GGG is derived from the separate forms of Helmholtz equations for each of the TE(E_{y0}, H_{x0}, H_{z0}) and TM(H_{y0}, E_{x0}, E_{z0}) modes, which are given as

$$\begin{aligned}
&\frac{\partial^2 E_{y0}}{\partial z^2} - \left[\beta^2 - \varepsilon_g\left(\frac{\omega}{c}\right)^2\right] E_{y0} = 0 \\
&\frac{\partial^2 H_{y0}}{\partial z^2} - \left[\beta^2 - \varepsilon_g\left(\frac{\omega}{c}\right)^2\right] H_{y0} = 0 \qquad (6)
\end{aligned}$$

where $\varepsilon_0\varepsilon_g$ is the dielectric constant of GGG.

Solutions to (6) are given under the boundary condition of the ground plane $z = -s$ with unknown constants B_1 and B_2

$$\begin{aligned}
E_{y0} &= B_1\sin\left[p_z(z+s)\right] \\
H_{y0} &= B_2\cos\left[p_z(z+s)\right] \\
p_z^2 &= \varepsilon_g\left(\frac{\omega}{c}\right)^2 - \beta^2. \qquad (7)
\end{aligned}$$

Due to the boundary condition at the interface between YIG and GGG at $z = 0$, tangential components of the electromagnetic field must be continuous. Eliminating unknown constants A_1 and A_2 in (5) and B_1 and B_2 in (7), the dispersion relation can be derived as

$$\begin{aligned}
&\{\varepsilon_g\lambda_p\lambda_m\tanh(\lambda_p d)\tanh(\lambda_m d) + \varepsilon_r q_z^2\tan^2(p_z s)\}\sqrt{D} \\
&\quad + \left[\left\{\varepsilon_g\frac{q_z^2}{p_z}\lambda_p\tanh(\lambda_p d) + \varepsilon_r p_z\lambda_m\tanh(\lambda_m d)\right\} C_m\right. \\
&\quad \left. - \left\{\varepsilon_r p_z\lambda_p\tanh(\lambda_p d) + \varepsilon_g\frac{q_z^2}{p_z}\lambda_m\tanh(\lambda_m d)\right\} C_p\right] \\
&\quad \times\tan(p_z s) = 0 \qquad (8)
\end{aligned}$$

where

$$\begin{aligned}
C_p &= \frac{(\mu-1)\beta^2 + \sqrt{D}}{2} \\
C_m &= \frac{(\mu-1)\beta^2 - \sqrt{D}}{2} \\
q_z^2 &= \varepsilon_g\left(\frac{\omega}{c}\right)^2 - \beta^2.
\end{aligned}$$

The dispersion relation was numerically solved. The numerical parameters used in the calculations are $\mu_0 H_0 = 0.057$ T, $\mu_0 M_0 = 0.175$ T, thickness of YIG film, $d = 20$ μm, thickness of GGG, $s = 400$ μm, $\varepsilon_r = 15.3$, and dielectric constant of GGG $\varepsilon_g = 7.7$.

Fig. 3 shows typical dispersion curves in a logarithmic scale of the propagation constant β, which reveals a mixed state of the magnetostatic forward volume wave (MSFVW) modes with a large propagation constant of over 500 rad/m and quasi-TEM modes having two resonances at $f_h = (\gamma\mu_0/2\pi)H_0$ and f_M'. It is interesting to note that the curve corresponding to the quasi-TEM mode joins the curve for the MSFVW mode at the gyromagnetic frequency f_h, which is clearly shown in the enlarged figure. Such coupling behavior has not been found for the dispersion relation under the magnetostatic approximation [9] and Hines' mode or edge-guide mode [11]. This indicates that the MSFVW mode can be excited easily by coupling with the quasi-TEM

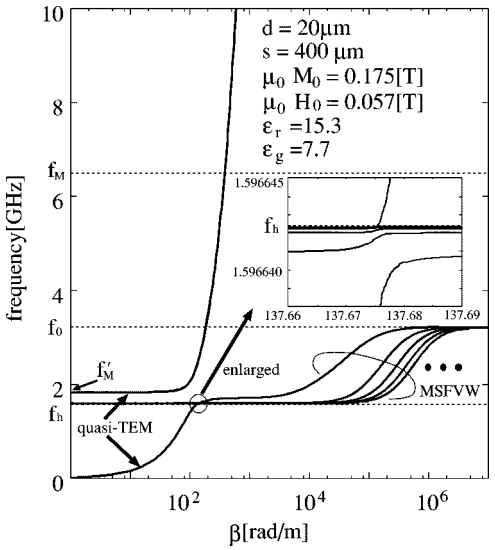

Fig. 3. Typical dispersion curve of the parallel-plate model of the strip line.

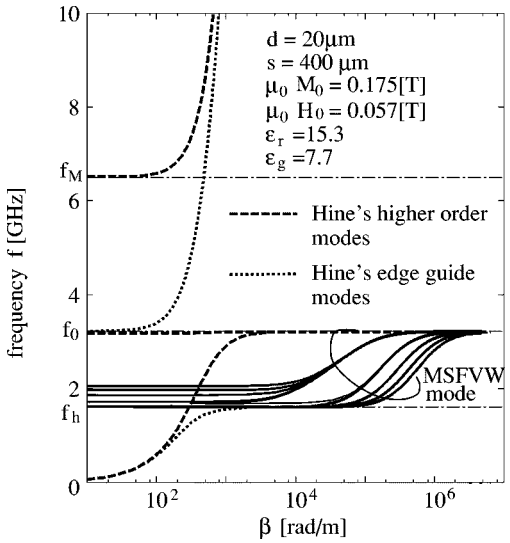

Fig. 4. Dispersion curves of the MSFVW under magnetostatic approximation and Hines' modes with three-dimensional model.

mode at $f = f_h$. It also means that the MSFVW soliton can be excited efficiently at f_h because the soliton formation can occur near the cutoff frequency of the MSFVW, i.e., f_h [3], [4]. The coupling coefficient value can be read from Fig. 3, a sufficiently accurate value to give perfect coupling between quasi-TEM and MSFVW modes for a YIG waveguide length of approximately a few centimeters, and no coupling between these modes was found without GGG substrate. On the other hand, the resonance frequency $f_M = (\gamma\mu_0/2\pi)(H_0 + M_0)$ moves to lower resonance frequency f'_M with the existence of the GGG substrate and with decreasing thickness of the YIG film, which is similar to the dispersion characteristics obtained by the spectral-domain method [12].

The effect of the width of the microstrip is interesting, but it may be a very complex problem because of the three-dimensional treatment of the line. When the magnetostatic approximation is assumed, the dispersion relation of the MSFVW mode in the three-dimensional model can be easily derived under the assumption of a perfect magnetic-wall boundary condition at the strip edge [9], which is also depicted in Fig. 4. Hines' mode, which is taken into consideration independent of the electromagnetic field in the direction perpendicular to the YIG-film–GGG structure, can also be easily derived from Maxwell's equation with a perfect magnetic-wall boundary at the strip edge [11], which is depicted in Fig. 4.

Comparing Figs. 3 and 4, the effect of the strip width on the dispersion curves is observed at two resonance frequencies $f_0 = (\gamma\mu_0/2\pi)\sqrt{H_0(H_0 + M_0)}$ and f_M. This is caused by Hines' higher order mode [11]. Except at the two resonance frequencies, the discrepancy between the dispersion curves in Figs. 3 and 4 is insignificant. The coupling between the two modes at f_h may be enhanced with change of the strip linewidth. Thus, the dispersion relation in the three-dimensional problem can be estimated from the two-dimensional dispersion relation. In addition, it can be emphasized that magnetostatic approximation is a powerful method, when we independently consider the MSFVW mode in the strip line.

On the other hand, the radiation of the MSFVW at the right angle to the proposed strip line has been used for excitation of the MSW, when we utilize the conventional transducer design of a narrow strip of width less than 100 μm [7], [8]. It has been confirmed experimentally that if the strip width is greater than a few tens of micrometers, the effect on the radiation of the MSFVW is small and does not disturb the transmission characteristic of the line [10].

III. Simulation of Soliton Form

The MSW envelope soliton in the YIG-film waveguide is a typical nonlinear phenomenon and shows the properties similar to optical solitons in fiber optics [13], but the short length of the waveguide is enough for forming MSW solitons [3], [4] compared to the long distance of optical fiber. To understand MSW envelope soliton behavior, the simulation study using the nonlinear Schrödinger equation (NLSE) is a popular method and the numerical parameters can be read from the linear state of the dispersion curve of the MSFVW discussed in Section II.

The NLSE is given by

$$j\left(\frac{\partial\varphi}{\partial y} + k'_\omega\frac{\partial\varphi}{\partial t} + k'_\omega\Gamma\varphi\right) - \frac{1}{2}k''_\omega\frac{\partial^2\varphi}{\partial t^2} + k'_{|\varphi|^2}|\varphi|^2\varphi = 0 \tag{9}$$

where k'_ω is the group velocity and k''_ω is the dispersion of the group velocity, which are numerically evaluated from the dispersion curve of MSFVW mode, as shown in Fig. 3. Γ is the loss, which corresponds to the linewidth of ΔH of the YIG film. Positive nonlinear coefficient of the dispersion $N = k'_{|\varphi|^2}$ cannot be read from the dispersion curve of the MSFVW mode of Fig. 3. However, N is easily evaluated from the demagnetizing factor due to the external dc magnetic field normal to the YIG film near f_h, the lower cutoff frequency of the MSFVW [3], [4].

The NLSE (9) can be numerically solved using the split-step Fourier-transform method [10]. Typical simulation results of soliton propagation are shown in Fig. 5 with and without loss

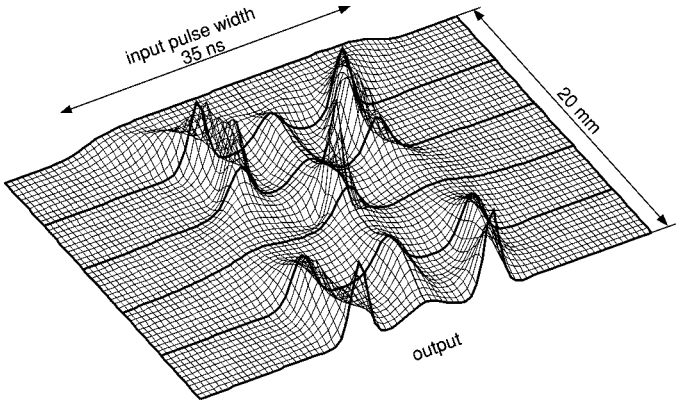

(a)

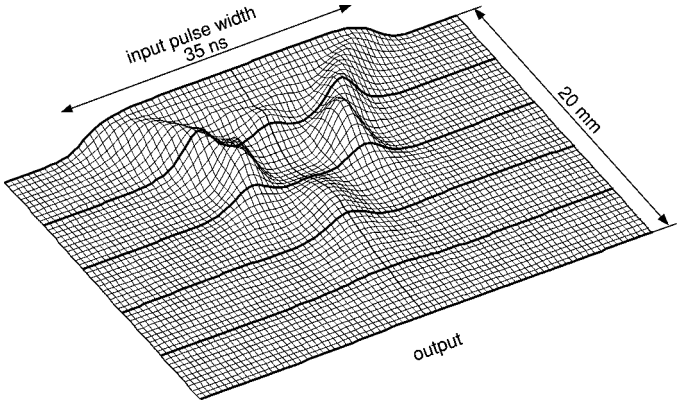

(b)

Fig. 5. Simulation results of soliton form with and without magnetic loss ΔH. (a) Without loss. (b) With loss.

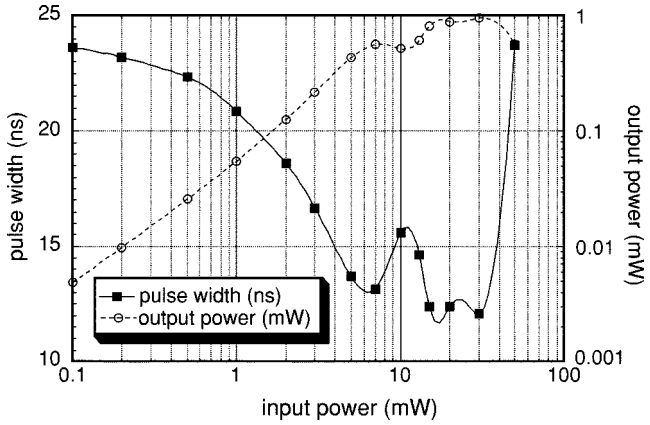

Fig. 6. Simulation results of the MSFVW soliton form in output pulsewidth and power.

ΔH, where numerical parameters of RF magnetization and the Poynting power for the NLSE calculation were taken from the dispersion curve of the MSFVW mode at 3.1 GHz in Fig. 3.

Fig. 5 shows that the output pulse takes the soliton form of a hyperbolic secant function even if loss in the waveguide is taken into account. The power dependence of the soliton form considering magnetic loss $\Delta H = 0.5$ Oe can be read from the simulated results in Fig. 5(b) and are plotted in Fig. 6 with the power dependence on amplitude and pulsewidth. It can be seen

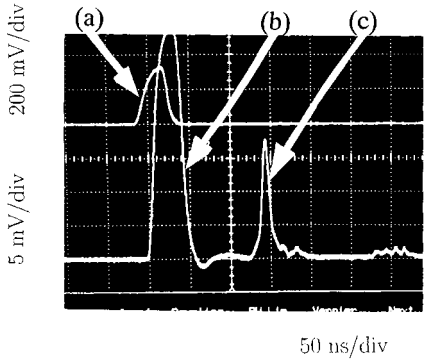

Fig. 7. (a) Photograph of input (input RF pulse signal (200 mV/div). (b) Zero-delayed signals (TEM signal (5 mV/div). (c) Output soliton signal (solition waveform (5 mV/div) at $\mu_0 H_0 = 0.275$ T).

from the figure that the output power of the MSFVW mode saturates at input power level of 10 mW and the pulsewidth is compressed up to 12 ns due to the formation of bright solitons; the input pulse is of 24-ns width with a power of 20 mW at 3.1 GHz.

IV. Experimental Results

The microstrip-type MSFVW delay line used for the experiment is shown in Fig 1(b). It consists of a 15 mm $\times$ 24 mm substrate with a 20-μm-thick YIG film with the magnetic loss $\Delta H \simeq 0.5$ Oe, and 400-μm-thick GGG. The 1-mm-wide strip line was fabricated on the substrate together with input and output ports. The dc magnetic field H_0 is applied normal to the YIG film to support the MSFVW mode along the microstrip lines. A microwave signal with frequency in the range of 2–4 GHz was modulated by a p-i-n diode modulator or GaAs FET switch with a 35-ns pulsewidth. The pulsed microwave signal was amplified up to 2 W by a GaAs high-power amplifier.

Fig. 7 shows: (a) typical waveforms of the input pulse; (b), the quasi-TEM signal with zero delayed time; and (c) the soliton form with 150-ns delayed time at an input power of 2 W at 3.2 GHz. By introducing an air gap in the stripline, the quasi-TEM mode shown in Fig. 7(b) can be suppressed sufficiently in the output signal.

Fig. 8 shows the input power dependence of the pulsewidth and amplitude of the output soliton pulse. The figure shows that the input pulse was compressed to 13 ns at the input power of 2 W, which represents a compression ratio of 2.7 for the input pulsewidth of 35 ns, and its amplitude shows limiter characteristics [10]. For input power higher than 2 W, the soliton form changes from one-soliton state to multisoliton state. The simulated result in Fig. 6 and the experimental result in Fig. 8 agree phenomenologically, but the real input power in the experiment cannot be reproduced because the conversion loss factor from the quasi-TEM to MSFVW mode in the strip line is unknown.

Fig. 9 shows some experimental results of soliton forms for double-input pulses at 3.3 GHz. Two pulses with closed form can be separated by the soliton operation, which may be useful for digital microwave signal processing.

Therefore, it was demonstrated that MSW envelope soliton could be observed in the microstrip-line-type delay line similar

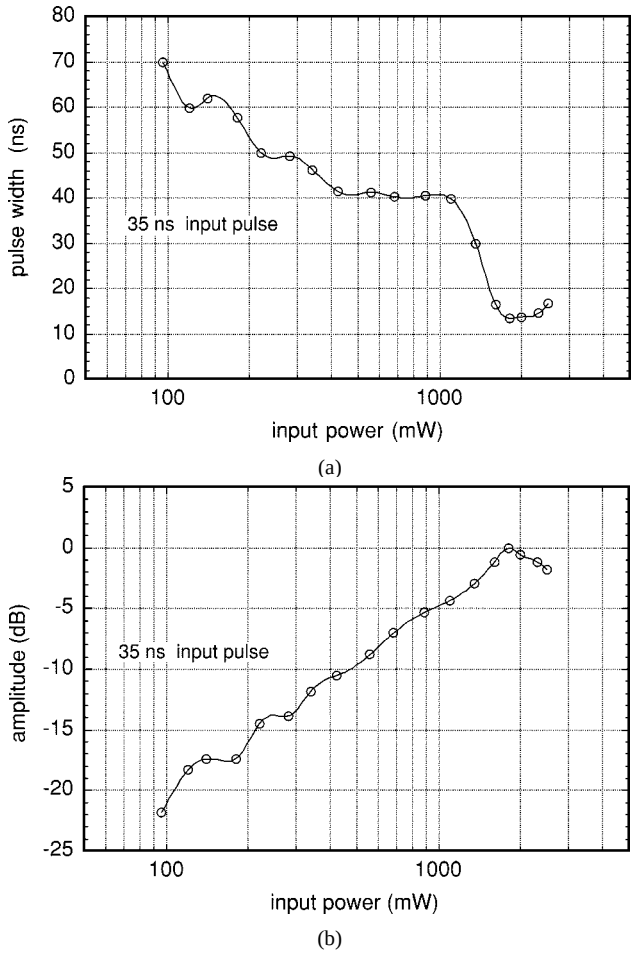

Fig. 8. Power dependence of pulsewidth and amplitude of output signal. (a) Soliton pulsewidth. (b) Soliton amplitude.

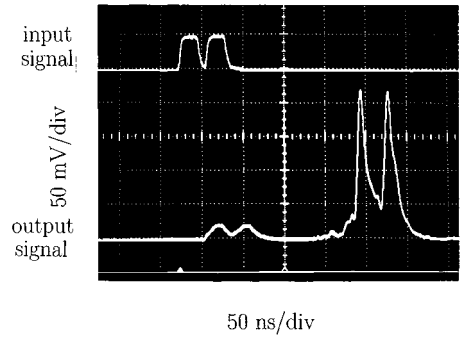

Fig. 9. Photograph of soliton form with input double pulses.

to the conventional MSW waveguide with a pair of microstrip transducers [2]–[4].

V. Conclusions

The dispersion relation was derived from a two-dimensional model of the microstrip line. The dispersion curves show the state of the quasi-TEM mode mixed with the MSFVW mode, and these two modes couple with each other at the gyromagnetic frequency, which is a very effective frequency for exciting solitons through $f_h = (\gamma\mu_0/2\pi)H_0$. The effect of the strip width is also discussed in terms of the MSFVW mode under a magnetostatic approximation, and imposing the magnetic-wall boundary condition, a deviation in the dispersion curve near the magnetic resonance frequency was observed.

The MSFVW envelope soliton was experimentally demonstrated in the strip line with YIG film on a GGG layered substrate. A short microwave pulse of 13 ns was obtained with an input pulse of 35 ns and 2 W at 3.2 GHz.

Simulation of the soliton form was carried out by numerical solution of the NLSE. The results were compared with the experiment and good agreement was found.

The nonlinear characteristics of the strip line on the YIG substrate, which exhibits soliton behavior, may be useful in designing microwave pulse compression devices [5], beamforming of antennas [14], limiters [15], and *S/N* enhancers operating at relatively low microwave power [16]. To realize these devices, analysis of dispersion relation of the strip line should include loss parameters of the YIG film.

References

[1] "Special section on microwave magnetics," *Proc. IEEE*, vol. 86, pp. 138–187, Feb. 1988.

[2] B. A. Kalinikos, N. G. Kovshikov, and A. N. Slavin, "Spin-wave envelope solitons in thin ferromagnetic films," *J. Appl. Phys.*, vol. 67, no. 9, pp. 5633–5638, May 1, 1990.

[3] M. A. Tsankov, M. Chen, and C. E. Patton, "Forward volume wave microwave envelope solitons in yttrium iron garnet films, propagation decay and collision," *J. Appl. Phys.*, vol. 76, no. 7, pp. 4274–4289, Oct. 1994.

[4] H. Y. Zhang, P. Kabos, H. Xia, R. A. Staudinger, P. A. Kolodin, and C. E. Patton, "Modeling of microwave magnetic envelope solitons in thin ferrite films through the nonlinear Schrödinger equation," *J. Appl. Phys.*, vol. 84, no. 7, pp. 3776–3785, Oct. 1998.

[5] V. Priye and M. Tsutsumi, "Observation of short pulse in cascaded magnetostatic soliton waveguide," *Electron. Lett.*, vol. 16, pp. 464–465, Mar. 1995.

[6] Y. K. Fetisov, P. Kabos, and C. E. Patton, "Active magnetostatic wave delay line," *IEEE Trans. Magn.*, vol. 34, pp. 259–271, Jan. 1998.

[7] S. N. Bajpai, "Suppression of higher-order thickness modes in magnetostatic forward volume wave delay lines," *J. Appl. Phys.*, vol. 59, no. 3, pp. 970–972, Feb. 1986.

[8] A. K. Gangury and D. C. Webb, "Microstrip excitation of magnetostatic surface waves: Theory and experiment," *IEEE Trans. Microwave Theory Tech.*, vol. MTT-23, pp. 998–1006, Dec. 1975.

[9] K. Okubo, V. Priye, and M. Tsutsumi, "A new magnetostatic wave delay line using YIG film," *IEEE Trans. Magn.*, vol. 33, pp. 2338–2341, May 1997.

[10] M. Tsutsumi, T. Ueda, and K. Okubo, "Nonlinear behavior of electromagnetic waves in the YIG film microstrip line," in *IEEE MTT-S Int. Microwave Symp. Dig.*, June 1998, pp. 841–844.

[11] M. E. Hines, "Reciprocal and nonreciprocal modes of propagation in ferrite stripline and microstrip devices," *IEEE Trans. Microwave Theory Tech.*, vol. MTT-19, pp. 442–451, May 1971.

[12] M. Tsutsumi and T. Asahara, "Microstrip lines using yttrium iron garnet film," *IEEE Trans. Microwave Theory Tech.*, vol. 38, pp. 1461–1467, Oct. 1990.

[13] J. R. Taylor, *Optical Solitons—Theory and Experiment*. Cambridge, U.K.: Cambridge Univ. Press, 1992.

[14] M. Tsutsumi and T. Ueda, "Characteristics of microstrip line on YIG film substrate and its application to beam forming of antenna," , to be published.

[15] J. D. Adam and S. N. Stitzer, "Frequency selective limiters for high dynamic range microwave receivers," *IEEE Trans. Microwave Theory Tech.*, vol. 41, pp. 2227–2231, Dec. 1993.

[16] T. Nomoto and Y. Matsushita, "A signal to noise enhancer using two MSSW filters and its application to noise reduction in DBS reception," *IEEE Trans. Microwave Theory Tech.*, vol. 41, pp. 1316–1321, Aug. 1993.

Makoto Tsutsumi (M'71–SM'97) was born in Tokyo, Japan, on February 25, 1937. He received the B. S. degree in electrical engineering from Ritsumeikan University, Kyoto, Japan, in 1961, and the M.S. and Ph.D. degrees in communication engineering from Osaka University, Osaka, Japan, in 1963 and 1971, respectively.

From 1984 to 1987, he was an Associate Professor of communication engineering at Osaka University. Since 1988, he has been a Professor in the Department of Electronics and Information Science, Kyoto Institute of Technology, Kyoto, Japan. His research interests are primarily in microwave and millimeter-wave ferrite devices and optics/microwave interactions in the semiconductor.

Tetsuya Ueda (M'97) was born in Hyogo, Japan, in 1969. He received the B.E., M.E., and Ph.D. degrees in electrical communication engineering from Osaka University, Osaka, Japan, in 1992, 1994, and 1997, respectively.

In 1997, he joined the Department of Electronics and Information Science, Kyoto Institute of Technology, Kyoto, Japan, where he is currently a Research Associate. His research interests are in nonlinear microwave ferrite devices and optical-microwave interaction in magnetooptic medium.

Kensuke Okubo (M'93) received the B.E., M.E., and D.Eng. degrees in electrical engineering from the Kyoto Institute of Technology, Kyoto, Japan, in 1987, 1989, and 1992, respectively.

In April 1993, he joined the Faculty of Computer Science and System Engineering, Okayama Prefectural University, Okayama, Japan, where he is currently an Associate Professor. His research interests are in microwave and millimeter-wave ferrite devices and the radio-wave image method.